

**A and A** Manuscript-Nr.  
(will be inserted by hand later)

**Your thesaurus codes are:**  
02.01.1, 09.03.2, 02.16.1, 08.19.4, 02.19.1

ASTRONOMY  
AND  
ASTROPHYSICS  
6.9.2018

# Cosmic Rays

## VII. Individual element spectra: prediction and data

**Barbara Wiebel-Sooth<sup>1</sup>, Peter L. Biermann<sup>2</sup>, and Hinrich Meyer<sup>1</sup>**

<sup>1</sup> Fachbereich Physik, Universität Wuppertal, Gaußstr. 20, D-42097 Wuppertal, Germany,

<sup>2</sup> Max Planck Institut für Radioastronomie, Auf dem Hügel 69, D-53121 Bonn, Germany

Received; accepted

**Summary.** Based on the earlier papers in this series, we discuss here the errors in the prediction of the model, and compare with the error ranges in the spectra for individual elements. The predictions are spectra of  $E^{-2.75 \pm 0.04}$  for hydrogen, and  $E^{-2.67 - 0.02 \pm 0.02}$  for helium and heavier elements below the knee. For particle energies above  $10 Z$  GeV the data give  $E^{-2.77 \pm 0.02}$  for hydrogen and  $E^{-2.64 \pm 0.02}$  for helium and similar values for all heavier elements combined, where  $Z$  is the charge of the nucleus considered. At the higher energy range considered here the secondary elements Li, Be, and B as well as the sub-Fe group have spectra consistent with source-related spallation, such as occurs when a supernova driven explosions runs into a shell around the wind of the predecessor star.

**Key words:** Acceleration of particles – Cosmic Rays – Plasmas – Supernovae: general – Shockwaves

### 1. Introduction

The origin of cosmic rays (Hess 1912, Kohlhörster 1913) is still one of the main enigmas of physics. Many energetic sources have been claimed to explain parts of the population of cosmic ray particles observed. Novae, pulsars, supernova explosions, stellar wind bubbles, interstellar turbulence, radio galaxies and many other sources have been explored (Fermi 1949, 1954; Peters 1959, 1961; Berezinsky et al. 1990).

#### 1.1. The origin of cosmic rays

Recently we have proposed that cosmic rays can be traced to three different source sites:

- 1 . Supernova explosions into the interstellar medium, or ISM-SNe. This component produces mostly hydrogen and the observed energetic electrons up to about 30 GeV, and dominates the *all particle* flux up to near  $10^4$  GeV.
- 2 . Supernova explosions into the predecessor stellar wind, wind-SNe. This component produces the observed energetic electrons above 30 GeV, and helium and most heavier

elements already from GeV particle energies. Due to a reduction in acceleration efficiency at a particular rigidity the slope increases, thus producing the knee feature. The component extends ultimately to several EeV. Since the winds of massive stars are enriched late in their life, this component shows a heavy element abundance which is strongly increased over the interstellar medium.

3 . Powerful radio galaxies produce a contribution which dominates beyond about 3 EeV, and consists mostly of hydrogen and helium, with only little addition of heavy elements below 50 EeV. At this energy the interaction with the microwave background cuts off the contribution from distant extragalactic sources, the Greisen-Zatsepin-Kuzmin (GZK) cutoff. There are a small number of events which appear to be beyond this energy, and whether they fit into such a picture is open at present.

The theory was originally proposed in Biermann (1993a, paper CR I) and in Rachen & Biermann (1993, paper UHE CR I). Various tests were performed in Biermann & Cassinelli (1993, paper CR II); Biermann & Strom (1993, paper CR III); Stanev et al. (1993, paper CR IV); Rachen & Biermann (1993, paper UHE CR I); Rachen et al. (1993, paper UHE CR II); Nath & Biermann (1993, 1994a, 1994b); Biermann et al. (1995a); Biermann et al. (1995b, paper CR V); Stanev et al. (1995); Biermann et al. (1997) and Biermann (1993b, c, 1994, 1995a, b, 1996, 1997a, 1997b).

In this paper we will at first briefly discuss the error determination of the theory in Sect. 2, then the data for individual elements in Sect. 3, compare and discuss secondary elements versus primary elements in Sect. 4, and conclude in Sect. 5.

### 2. Errors inherent in the theory

#### 2.1. Basic concept

We consider the acceleration of particles in spherical shocks with the concept of first order Fermi acceleration (see, e.g., Drury 1983). In this concept energetic particles are cycling back and forth across the shock region, gaining energy each time they turn back; since the two sides of a shock are a permanently compressing system the particles gain energy. In a spherical shock the particles also lose energy from adiabatic expansion. Furthermore, in a system where the unperturbed

magnetic field is perpendicular to the shock normal, particles can modify their energy by drifts, here dominated by curvature drifts; the particles move sideways in a curved magnetic field, and experience an electric field from the motion through a magnetic field; the component of the motion parallel to the perceived electric field leads to an energy change. It has to be noted that for plane parallel shocks the drifts have been shown by Jokipii (1982) to be equivalent in their effect to the Lorentz transformation; here we emphasize that we use the curvature and gradient drifts only, which give an additional effect. A key ingredient in such an approach is the time spent by a particle on either side of the shock. Observations as well as stability arguments lead us to the notion, that the time spent on either side of the shock is given by a transport coefficient  $\kappa$  given by fast convective motion (see Biermann 1993a, 1997b). The construction of this transport coefficient is the major step in the argument, and is based on the concept of the *smallest dominant scale*, a scale either in real space or in phase space. The resulting expression for the spectrum of the energetic particles is the same as in, e.g., Drury (1983), except for an additional term for energy gains from drifts (Jokipii 1987).

For the expansion of a spherical shock into a stellar wind we adopt the basic magnetic configuration of a Parker spiral (Parker 1958, Jokipii et al. 1977), where the magnetic field in the equatorial plane is an Archimedian spiral with  $B_\phi$  dominating over  $B_r$ , decreases with  $B_\phi \sim (\sin \theta)/r$  towards the pole and outwards with radius  $r$ , and becomes mostly radial in the pole region. We write for the wind velocity  $V_W$ , for the shock velocity  $U_1$ , and for the downstream gas velocity in the shock frame  $U_2$ .

## 2.2. Assumptions and Systematic Uncertainties

The assumptions adopted are inspired by Prandtl's mixing length approach (Prandtl 1925, 1949); all use the key proposition that the **smallest dominant scale**, either in geometric length, or in velocity space, gives the natural transport coefficient. In this sense the assumptions are *derived from a basic principle*.

Our basic, **argument 1**, *based on observational evidence as well as theoretical arguments*, is that for a cosmic ray mediated shock the *convective random walk* of energetic particles perpendicular to the *unperturbed* magnetic field can be described by a diffusive process with a downstream diffusion coefficient  $\kappa_{rr,2}$  which is given by the thickness of the shocked layer and the velocity difference across the shock, and is independent of energy.

The upstream diffusion coefficient can be derived in a similar way, but with a larger scale based on the *same column density as in the downstream layer*. This leads to the second critical, **argument 2**, namely that the upstream length scale is just  $U_1/U_2$  times larger.

It must be remembered that there is a lot of convective turbulence which increases the curvature: The characteristic scale of the turbulence is  $r/4$  for strong shocks, again, as an example, in the case of the wind-SN, and thus the curvature is  $4/r$  maximum. Half the maximum of the curvature allows for the net balance of gains and losses for the energy gain due to drifts (**argument 3**), and so we obtain then for the curvature  $2/r$  which is twice the curvature without any turbulence; this increases the curvature term for the spectral range below the knee.

The diffusion tensor component  $\kappa_{\theta\theta}$  can be derived similar to our heuristic derivation of the radial diffusion term  $\kappa_{rr}$ , again by using the smallest dominant scales. The characteristic velocity of particles in  $\theta$  is given by the erratic part of the drifting, corresponding to spatial elements of different magnetic field direction, and this is on average the value of the drift velocity  $|V_{d,\theta}|$ , possibly modified by the locally increased values of the magnetic field strength, and the characteristic length is the distance to the symmetry axis  $r \sin \theta$  (**argument 4**); this is the smallest dominant scale as soon as the thickness of the shocked layer is larger than the distance to the symmetry axis, i.e.  $\sin \theta < U_2/U_1$ .

Rapid convection also gives a competing diffusion in the  $\theta$ -direction, independent of particle energy; this will begin to dominate as soon as the energy dependent  $\theta$ -diffusion coefficient reaches this maximum at a critical energy. As long as the  $\theta$ -diffusion coefficient is smaller, it will dominate particle transport in  $\theta$  and the upper limit derived here is irrelevant. When the  $\theta$ -diffusion coefficient reaches and passes this maximum given by the fast convection, then the particle in its drift will no longer see an increased curvature due to the convective turbulence due to averaging and the part of drift acceleration due to increased curvature is eliminated. Again, a detailed consideration of gains and losses of the drift energy gains leads to the spectrum of particles beyond the knee. The critical energy derived in this way is the same as that derived from a phase-space argument near the poles.

All these arguments are inspired by Prandtl's mixing length approach; all use the key proposition that the **smallest dominant scale**, either in geometric length, or in velocity space, gives the diffusive transport discussed. We assume this to be true even for the anisotropic transport parallel and perpendicular to the shock.

We emphasize the analogy to simple limiting scaling arguments such as a) the estimate of the temperature gradient in the lower hydrogen convection zone on the Sun, which is followed by nature to a very good approximation (Strömgren 1953, p. 65), and b) the estimate of the Kolmogorov turbulence spectrum (Rickett 1990, Goldstein et al. 1995), which appears to be also followed by nature in many sites over many orders of magnitude in length scale. Whether the cosmic rays follow also such a limiting scaling argument, as regards their spectrum, to such an accuracy remains to be seen. This paper is a step to verify the straight forward prediction for 28 chemical elements individually.

In addition, we i) use the simplified notion of a purely spherical shock; ii) ignore the modifications of the shock introduced by the cosmic rays themselves, except in the conceptual derivation of the initial argument, where the cosmic rays are critical for the instability; and iii) use a test particle approach.

We have to emphasize very strongly that these uncertainties mean that the spectral indices derived for the powerlaw region of the various components of the cosmic rays correspond to a limiting argument: If things were really as simple - and they are likely to be much more complicated - then the spectrum derived and any comparison with data has to be taken with considerable caution.

On the other hand, the very simplicity of the proposed concept makes it easier to test and this is what we propose to do.

### 2.3. The error budget

#### 2.3.1. Below the knee

As discussed in paper CR III, the simplifications which we did make in treating the flow field of the expansion of a supernova explosion into the interstellar medium lead to an uncertainty of  $\pm 0.04$  in spectral index.

For wind-supernovae we can estimate one uncertainty, which arises from the finite wind speed of Wolf Rayet stars, or those massive stars with strong winds which explode as supernovae. These wind speeds can go up to several thousand km/sec, while the supernova shock is variously estimated to  $10^4$  km/sec to twice that much. As a limiting argument we use that the ratio of the wind speed to the supernova shock speed is  $< 0.2$ ; this gives a steepening of the derived spectral index of the particle distribution by 0.04. This uncertainty also may correspond to curvature of the spectrum, since there is a time-evolution as the shock progresses out through the stellar wind: As more energy of the shock is dissipated and more mass of the stellar wind snowplowed, the shock slows down; then those particles already accelerated keep their flatter spectrum (see Eq. 2.44 of Drury 1983), while those particles freshly injected and accelerated will have a steeper spectrum. Thus, in the range  $V_W/U_1 = 0, \dots, 0.2$  we obtain a spectral index in the range  $7/3, \dots, 7/3 + 0.04$ . Therefore we ascribe to the spectral index derived here an uncertainty of  $0.02 \pm 0.02$ , which describes both the uncertainty in an assumed powerlaw, and the possible curvature. This way of writing makes it clear that we *do not* expect the distribution of observed spectral indices to follow a gaussian distribution, but rather to be biased towards faster winds, which steepen the spectrum.

#### 2.3.2. The knee

In the Fermi-acceleration process there is energy gain and energy loss in each cycle which an energetic particle crosses the shock region; one part of this energy gain is due to drifts. At a certain rigidity ( $\sim E/Z$ ) the drift contribution is reduced, and so the slope of the spectrum changes. This critical energy is given by

$$E_{knee} = ZeB(r)r\left(\frac{3}{4}\frac{U_1}{c}\right)^2. \quad (1)$$

In a Parker-wind the product of radius  $r$  and magnetic field strength  $B(r)$  is a constant with radius.  $Z$  is the charge of the particle and  $e$  is the electromagnetic charge unit.  $U_1$  is the advance speed of the shock caused by the supernova explosion;  $U_2 = U_1/4$ .

This implies that the chemical composition at the knee changes so, that the gyroradius of the particles at the spectral break is the same, implying that the different nuclei break off in order of their charge  $Z$ , considered as particles of a certain energy (and not as energy per nucleon). In an all-particle spectrum in energy per particle, this introduces a considerable smearing.

There is one additional cosmic ray component from that latitude region near the pole of the magnetic field structure in the wind, where the magnetic field is predominantly radial rather than tangential. This region we call the polar cap. Thus the spectrum is harder in the polar cap region, because we are close to the standard parallel shock configuration, for which the particle spectrum is well approximated by  $E^{-2}$  at the source.

Because of spatial limitations most of the hemisphere has to dominate again above the knee, although with a fraction of the hemisphere that decreases with particle energy. This introduces a weak progressive steepening of the spectrum with energy. The superposition of such spectra for different chemical elements, including the polar cap contribution, has been tested (see paper CR IV). The results of these checks suggest that the polar cap may be the source for the flattening of the cosmic ray spectrum as one approaches the knee feature.

We note that we are using a limiting argument to derive the spectrum below the knee, and again use a limiting argument (see below) for the spectrum above the knee. Close to the knee, such an argument breaks down on either side, and so a softening of the knee feature is to be expected. On top of such a softened knee feature the polar cap is an additional component.

The expression for the particle energy at the knee also suggests by the clearly observed break of the spectrum that the actual values of the combination  $B(r)rU_1^2$  must be limited in range for all supernovae that contribute appreciably in this energy range. We have speculated on possible reasons for such a behaviour elsewhere (paper CR I, and in Biermann 1995a). We note that the recent results from the Tibet array suggest that the knee may in fact be rather smooth (Amenomori et al. 1996), in apparent contrast to the earlier description of the Akeno data (Nagano et al. 1984; see also Stanev et al. 1993).

#### 2.3.3. Beyond the knee

Beyond the knee, the drift contribution to the cyclical energy gain of individual particles is reduced, and so we obtain a steeper spectrum with an error which we write as  $0.07 \pm 0.07$ . As noted above the use of limiting arguments to derive the spectrum on either side of the knee implies that the knee itself may be quite soft, and thus curvature is to be expected.

#### 2.3.4. The ultimate cutoff

The maximum energy particles can reach depends linearly on the magnetic field

$$E_{max} = ZerB(r). \quad (2)$$

If stars that explode as wind-supernovae were to vary widely in their magnetic field strength, then this maximum energy would also vary from star to star, and as a result the sum of all contribution would appear as strongly curved downwards.

### 2.4. The predictions

The proposal is that three sites of origin account for the cosmic rays observed, i) supernova explosions into the interstellar medium, ISM-SN, ii) supernova explosions into the stellar wind of the predecessor star, wind-SN, and iii) radio galaxy hot spots for the extragalactic component. Here the cosmic rays attributed to supernova-shocks in stellar winds, wind-SN, produce an important contribution at all energies up to  $3 \cdot 10^9$  GeV.

Particle energies go up to 100 Z TeV for ISM-SN, and to 100 Z PeV with a bend at 600 Z TeV for wind-SN. Radiogalaxy hot spots may go up to near 1000 EeV at the source. These

numerical values are estimates with uncertainties of surely larger than a factor of 2, since they derive from an estimated strength of the magnetic field, and estimated values of the effective shock velocity (see above).

The spectra  $\Phi(E)$  are predicted to be

$$\Phi_{ISM}(E) \sim E^{-2.75 \pm 0.04} \quad (3)$$

for ISM-SN (paper CR III), and

$$\Phi_{wind}(E) \sim E^{-2.67 - 0.02 \pm 0.02} \quad (4)$$

for wind-SN below the knee,  $E^{-3.07 - 0.07 \pm 0.07}$  for wind-SN above the knee, and  $E^{-2.0}$  at injection for radiogalaxy hot spots. The polar cap of the wind-SN contributes an  $E^{-2.33}$  component (allowing for leakage from the Galaxy), which, however, contributes significantly only near and below the knee, if at all.

The chemical abundances are near normal for the injection from ISM-SN, and are strongly enriched for the contributions from wind-SN.

This means that the sources for cosmic ray particles and the sources for the enrichment of the interstellar medium are the same, and hence it is no surprise that the isotopic ratios are similar for galactic cosmic ray sources and the solar system (DuVernois et al. 1996a, 1996b).

That spallation-produced secondaries require a strongly enriched original composition has been confirmed by a calculation of the formation of light elements in the early Galaxy and a comparison with observed abundances (Ramaty et al. 1997); we consider this to be an important check on the picture proposed here.

At the knee the spectrum bends downwards at a given rigidity, and so the heavier elements bend downwards at higher energy per particle. Thus beyond the knee the heavy elements dominate all the way to the switchover to the extragalactic component, which is, once again, mostly Hydrogen and Helium, corresponding to what is expected to contribute from the interstellar medium of a radiogalaxy, as well as from any intergalactic contribution mixed in (Biermann 1993c). This continuous mix in the chemical composition at the knee already renders the overall knee feature in a spectrum in energy per particle unavoidably quite smooth, a tendency which can only partially be offset by the possible polar cap contribution, since that component also is strongest at a given rigidity (for details see the discussion in paper CR IV). This is confirmed by Amenomori et al. (1996). They determined a spectral index of  $-2.60 \pm 0.04$  below the knee and  $-3.00 \pm 0.05$  above the knee with the slope changing continuously between  $10^{14.75}$  eV and  $10^{15.85}$  eV.

We note that uncertainties of the spectrum derive from a) the time evolution of any acceleration process as the shock races outward, b) the match between ISM-SN and wind-SN, c) the mixing of different stellar sources with possibly different magnetic properties, and d) the differences in propagation in any model which uses different source populations. These uncertainties translate into a distribution of powerlaw indices of the spectra, to curvature of the spectra, to a smearing of the knee feature, and to a smoothing of the cutoffs. Obviously, this is in addition to the underlying uncertainty associated with the concept of the *smallest dominant scale* itself.

### 3. The data

Here we describe the basic data set as available in the literature for individual elements, give several plots, and tables. The sources for the data are given in Table 4 of the Appendix. The spectra have been fitted above an energy of  $10Z$  GeV, where  $Z$  is the charge of the nucleus, in order to minimize the effect of solar modulation; we repeated the exercise with 20 and  $30Z$  GeV as the lower boundary without finding a significant change (see, e.g. Garcia-Munoz et al. 1986; Evenson & Meyer 1984; Seo et al. 1991). The numbers given in the tables are from the first boundary above. For the fit we have used the CERN-library (MINUIT - Function Minimization and Error Analysis, CERN Program Library D506). The spectra fitted are of the form

$$\Phi = \Phi_0 (E/\text{TeV})^{-\gamma} (\text{m}^2 \text{ sec sr TeV})^{-1}, \quad (5)$$

where  $E$  is the energy per particle.

Table 1

Element	Z	$\Phi_0$	$\gamma$	$\chi^2/\text{df}$
H	1	$(11.51 \pm 0.41) 10^{-2}$	$2.77 \pm 0.02$	0.70
He	2	$(7.19 \pm 0.20) 10^{-2}$	$2.64 \pm 0.02$	2.63
Li	3	$(2.08 \pm 0.51) 10^{-3}$	$2.54 \pm 0.09$	0.90
Be	4	$(4.74 \pm 0.48) 10^{-4}$	$2.75 \pm 0.04$	0.37
B	5	$(8.95 \pm 0.79) 10^{-4}$	$2.95 \pm 0.05$	0.45
C	6	$(1.06 \pm 0.01) 10^{-2}$	$2.66 \pm 0.02$	1.42
N	7	$(2.35 \pm 0.08) 10^{-3}$	$2.72 \pm 0.05$	1.91
O	8	$(1.57 \pm 0.04) 10^{-2}$	$2.68 \pm 0.03$	1.70
F	9	$(3.28 \pm 0.48) 10^{-4}$	$2.69 \pm 0.08$	0.47
Ne	10	$(4.60 \pm 0.10) 10^{-3}$	$2.64 \pm 0.03$	3.14
Na	11	$(7.54 \pm 0.33) 10^{-4}$	$2.66 \pm 0.04$	0.36
Mg	12	$(8.01 \pm 0.26) 10^{-3}$	$2.64 \pm 0.04$	0.10
Al	13	$(1.15 \pm 0.15) 10^{-3}$	$2.66 \pm 0.04$	1.24
Si	14	$(7.96 \pm 0.15) 10^{-3}$	$2.75 \pm 0.04$	0.10
P	15	$(2.70 \pm 0.20) 10^{-4}$	$2.69 \pm 0.06$	0.68
S	16	$(2.29 \pm 0.24) 10^{-3}$	$2.55 \pm 0.09$	0.44
Cl	17	$(2.94 \pm 0.19) 10^{-4}$	$2.68 \pm 0.05$	2.36
Ar	18	$(8.36 \pm 0.38) 10^{-4}$	$2.64 \pm 0.06$	0.45
K	19	$(5.36 \pm 0.15) 10^{-4}$	$2.65 \pm 0.04$	4.58
Ca	20	$(1.47 \pm 0.12) 10^{-3}$	$2.70 \pm 0.06$	0.60
Sc	21	$(3.04 \pm 0.19) 10^{-4}$	$2.64 \pm 0.06$	0.81
Ti	22	$(1.13 \pm 0.14) 10^{-3}$	$2.61 \pm 0.06$	5.67
V	23	$(6.31 \pm 0.28) 10^{-4}$	$2.63 \pm 0.05$	6.83
Cr	24	$(1.36 \pm 0.12) 10^{-3}$	$2.67 \pm 0.06$	3.41
Mn	25	$(1.35 \pm 0.14) 10^{-3}$	$2.46 \pm 0.22$	5.38
Fe	26	$(1.78 \pm 0.18) 10^{-2}$	$2.60 \pm 0.09$	1.81
Co	27	$(7.51 \pm 0.37) 10^{-5}$	$2.72 \pm 0.09$	1.13
Ni	28	$(9.96 \pm 0.43) 10^{-4}$	$2.51 \pm 0.18$	5.47

We note that the spectral fit takes the experimental errors as given by the original authors into full account. The fairly small final error is just due to the assembly of all existing data and their critical combination. We have divided the results

into three tables. Table 1 gives the results from experiments where the elements can be separated. Table 2 gives the results where groups of elements have been measured together. Table 3 gives the results where we have added the data for groups of elements together, both based on individual measurements as well as from grouped measurements. In addition the spectral indices for the various elements as a function of nuclear charge number  $Z$  are shown in Fig. 1.

The data for He illustrate systematic errors in the normalization of the flux: the lower energy data by Seo et al. (1991) give a spectral index of  $2.68 \pm 0.03$ , here we obtain  $2.64 \pm 0.02$ , which is quite consistent. The graphs in Biermann et al. (1995a) clearly show that the slopes of the spectra of He for individual measurement campaigns agree, while their overall normalization is different. When combining data from different measurement techniques and campaigns this can lead to erroneous spectral indices, since different experiments cover different energy ranges. For example, when we apply the fit by omitting the data of Ryan et al. (1972), we obtain a spectral index for He of  $2.65 \pm 0.02$ .

**Table 2**

Element	$Z$	$\Phi_o$	$\gamma$	$\chi^2/df$
Ne - S	10 - 16	$(3.34 \pm 0.18) 10^{-2}$	$2.69 \pm 0.03$	4.02
Cl - Ca	17 - 20	$(3.35 \pm 0.15) 10^{-3}$	$2.74 \pm 0.03$	0.35
Sc - Mn	21 - 25	$(4.23 \pm 0.10) 10^{-3}$	$2.77 \pm 0.04$	2.04
Fe - Ni	26 - 28	$(1.97 \pm 0.10) 10^{-2}$	$2.62 \pm 0.03$	0.12

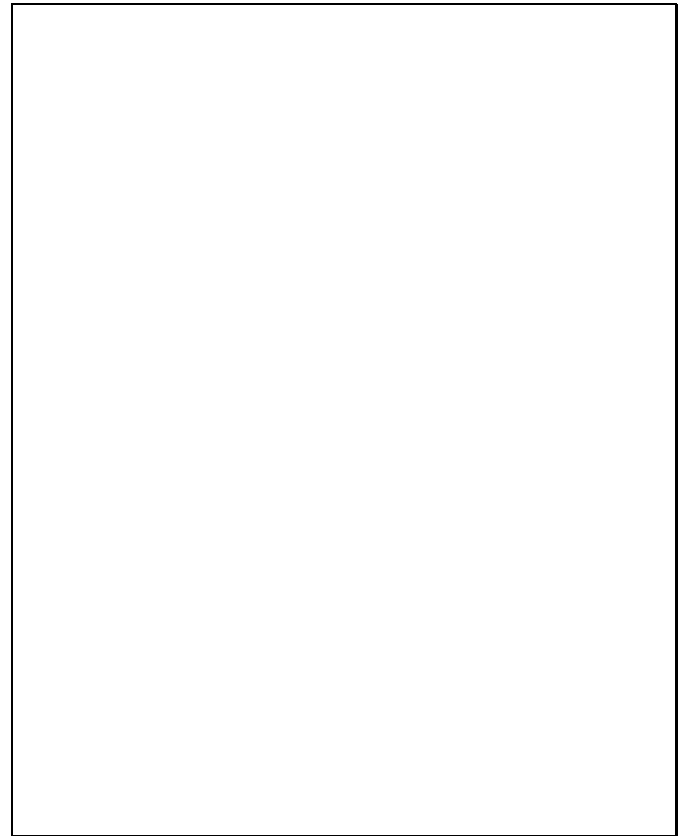
Table 2 shows the results of the fits in the case when experiments measured groups of elements directly. The comparison of Table 1 and 2 illustrates systematic errors still inherent in the data; for instance the individual elements Cl to Ca have all been measured by Engelmann et al. (1985, 1990), with Ca also measured by Ichimura et al. (1993a, b, c) and Kawamura et al. (1990). The group of elements Cl to Ca has been measured by Simon et al. (1980), Asakimori et al. (1991), Burnett et al. (1990a, b), JACEE (1993), and Ichimura et al. (1993a, b, c). Thus the two data sets are independent and allow to estimate errors. The difference illustrates that the systematic errors can be larger than the statistical errors, and that any agreement between spectral indices of prediction and data, as well as data for different elements has to be taken with some caution. In view of the diversity of the various experiments that contribute to the individual element spectra and the difficulties to give correct estimates of the systematic uncertainties, we consider the values for  $\chi^2/df$  obtained for the simple powerlaw fits as quite satisfactory. With this in view we combine elements to determine the power law parameters for groups of elements as shown in Table 3.

Table 3 shows the fits to all data available for the various groupings. We note that the particle spectra are close to the prediction: for hydrogen the prediction was  $2.75 \pm 0.04$ , and the data give  $2.77 \pm 0.02$ ; for the heavier elements He through Ni the prediction was  $2.67 + 0.02 \pm 0.02$ , and the data give  $2.64 \pm 0.04$ .

**Table 3**

Element	$Z$	$\Phi_o$	$\gamma$
low	1 - 2	$(18.81 \pm 0.76) 10^{-2}$	$2.71 \pm 0.02$
Li - B	3 - 5	$(3.49 \pm 0.40) 10^{-3}$	$2.72 \pm 0.06$
Be + B	4 - 5	$(1.36 \pm 0.11) 10^{-3}$	$2.90 \pm 0.04$
medium	6 - 8	$(2.86 \pm 0.06) 10^{-2}$	$2.67 \pm 0.02$
high	10 - 16	$(2.84 \pm 0.19) 10^{-2}$	$2.66 \pm 0.03$
very high	17 - 26	$(1.34 \pm 0.09) 10^{-2}$	$2.63 \pm 0.03$
Sc - Mn	21 - 25	$(4.74 \pm 0.20) 10^{-3}$	$2.63 \pm 0.03$
Fe - Ni	26 - 28	$(1.89 \pm 0.10) 10^{-2}$	$2.60 \pm 0.04$
He - Ni	2 - 28	$(15.80 \pm 1.35) 10^{-2}$	$2.64 \pm 0.04$
allparticle	1 - 28	$(27.47 \pm 2.43) 10^{-2}$	$2.68 \pm 0.02$

We conclude that despite the many simplifications in the theoretical approach the data are quite consistent with the predictions.



**Fig. 1.** The spectral indices for the various elements as a function of the nuclear charge number  $Z$ . The dashed lines indicate the range of the spectral index predicted for wind-SN.

We note that for the Fe-group elements we have *ignored* here the spallation correction from interaction in the interstellar medium, which produces a slight flattening; although not significant, the data are consistent with such a moderate flattening of these nuclei.

#### 4. The spectra of secondaries

Secondaries are produced when heavy nuclei break up in collisions with thermal nuclei, mostly hydrogen in the interstellar medium. If the production is throughout the time of transport then the secondaries are expected to show a steeper spectrum; if on the other hand the spallation is mostly already in the source region, then the secondary spectrum ought to be the same as that of the primaries.

The theory for the transport and the production of secondaries is well developed (e.g. Garcia-Munoz et al. 1987), and uses the steady state leaky box model to describe the spectrum as well as the secondary production; a recent review and summary of the problems inherent in this endeavor has been given by Shibata (1995). In a steady state leaky box model the ratio of the spectra of the secondary elements to the primary elements such as the boron/carbon or the sub-Fe/Fe ratio directly give the energy dependence of the diffusion time scale out of the Galaxy. Such a calculation gives an energy dependence for the time scale of  $\sim E^{-0.6}$  (e.g. Engelmann et al. 1990); one difficulty with this result is that it would lead to anisotropies of the cosmic rays and would not allow a direct extrapolation to energies beyond the knee. There is no other evidence for the relatively small scales in the interstellar medium of any turbulence other than consistent with a Kolmogorov spectrum, and also there is no evidence for a particular length scale corresponding to the Larmor radius at the knee. Therefore, we have proposed (Biermann 1996, 1997b), that the production of secondaries has three independent stages:

a) First of all, the giant molecular clouds themselves have a time evolution which cannot be neglected; they form out of smaller cloudlets faster than the Alfvénic time scale, and so *trap* the cosmic ray particles. These particles then leak out, with an energy dependence given by the Alfvénic turbulence in the cloud. We note that this corresponds to length scales far below what can be directly inferred from high angular resolution observations in clouds. Assuming that this turbulence also corresponds to a Kolmogorov spectrum (see, e.g., Goldstein et al. 1995), we then have a production rate of secondaries, which itself is a function of energy, and decreases with energy as  $E^{-1/3}$ . These particles are then released into the interstellar medium, where they are subject to diffusion out of the Galaxy, and so acquire another energy dependence of again  $E^{-1/3}$ , so as to give a total energy dependence of the secondary to primary ratio of  $E^{-2/3}$ , very close to that observed. This is of course limited to that energy range where diffusion is a useful concept in clouds, and when the time scale of diffusion is actually significantly shorter than the lifetime of the giant molecular cloud. Thus there is a critical energy per particle, which we estimate to near 20 Z GeV, above which this process becomes irrelevant. The detailed analytical derivation of this argument is given in full in Biermann (1996), and will be expanded upon in further communications.

b) Above this critical energy of an estimated 20 Z GeV, the Galaxy and its molecular clouds behave as stationary targets for cosmic ray interaction, and we come back to the canonical model, such as explained in Garcia-Munoz et al. (1987). Therefore, for these particles the secondary to primary ratio just acquires the energy dependence of interstellar turbulence, and so the ratio is expected to be  $\sim E^{-1/3}$ . This dependence is a smooth continuation of the steeper dependence at lower energies.

c) There is an additional contribution, which arises from the source, and which should be energy independent: As shown in Nath & Biermann (1994b) supernovae that explode into winds, hit a surrounding molecular shell, and then produce secondaries with an approximate grammage of order 1 - 3 gm/cm<sup>2</sup> (= column density traversed in the zig-zag path of charged particles in an inhomogeneous magnetic field). This then leads to a ratio of secondaries to primary particles which is energy independent, an aspect that has also been remarked by others (Drury et al. 1993).

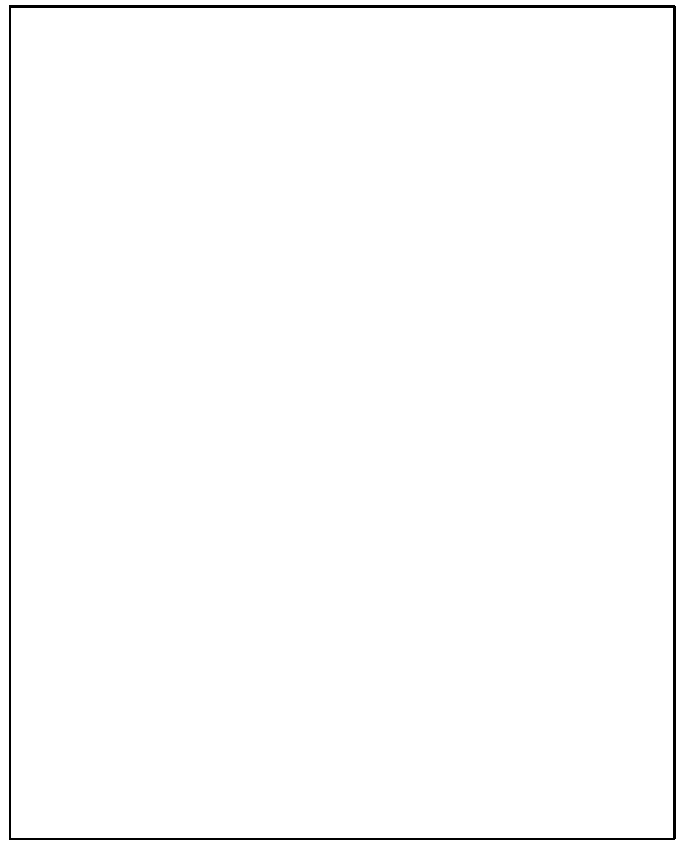


**Fig. 2.** Here we show the data as given by Shibata (1995), and fit them with the two models explained. The top shows the combination of process (a) and (b), and the bottom shows the combination of processes (a) and (c). (For explanation see text, Sect. 4)

We note that the ratio of these processes depends on the spallation cross section of the element considered; the relative strength of process (c) versus process (b) clearly depends on the element. For primary elements whose spallation cross section corresponds approximately to the effective grammage of process (c), the spallation of such an element is strongly affected by this process, while the spallation in the much higher grammage of processes (a) and (b) would then proceed to also influence the first generation secondaries, so as to finally produce secondaries of many generations down the element sequence.

Translating this result into the language common in the literature, this means that escape length as measured in gm/cm<sup>2</sup> and escape time can no longer be used synonymously. The escape time is proportional to  $E^{-1/3}$  in the relativistic range

of particle energies. The escape length as a means to describe interaction has three different regimes, and the one relevant in the GeV/nucleon range is about  $E^{-0.6}$ , and here, in our simplistic model,  $\sim E^{-2/3}$ .

All three contributions (a), (b), and (c) can be looked for in the data; the data are normally shown as *escape length*, which basically is the energy dependence of the secondary to primary ratio in the steady state leaky box model (see, e.g., Fig. 20 in Shibata 1995). With our model we can plot the same data as Shibata (1995) and can check whether we can fit either process (a) above combined with process (b), or process (c). We do this in Fig. 2.

In the first model combination (process (a) and (b)) we can satisfactorily fit the data with a grammage of about 19.8 gm/cm<sup>2</sup> for process (a) and a grammage of about 6.6 gm/cm<sup>2</sup> for process (b); the transition rigidity would be at  $27 \pm 5$  GV.

In the second model combination (process (a) and (c)) we can also satisfactorily fit the data with a grammage of about 29 gm/cm<sup>2</sup> for process (a), rather close to canonical values, and a grammage of  $\approx 1$  gm/cm<sup>2</sup> for process (c).

A judgement which model combination is a better to the data overall will be made below. The result is that model combination (a) and (c) appears to match the high energy data better for secondary elements; this means that spallation in time-dependent molecular clouds and in the molecular shells around massive star winds are the dominant contributors to the spallation observed.

We note again, as already emphasized in paper CR I that we use a turbulence spectrum in the interstellar medium, which has a single powerlaw over the entire range of length scales relevant for cosmic ray scattering, corresponding to energies up to a few EeV, and have argued that such a powerlaw is best approximated by a Kolmogorov law (Wiebel-Sooth et al. (1995); Wiebel-Sooth et al. (paper CR VI), in prep.; Biermann (1997b)).

#### 4.1. The elements Li, Be and B

The nuclei lithium, beryllium, and boron in energetic cosmic rays are produced mostly from the breakup of carbon and oxygen nuclei. The combined spectrum is shown in Fig. 3.

We note that the spectrum has a fairly large error range, but is quite consistent with a source-related component. However, the individual spectrum of Boron suggests a steepening by  $\approx 1/3$ , and so may be consistent with process (b), the spallation in clouds at energies which are so high as to render the time evolution of clouds irrelevant. On the other hand, the error bars for all three elements are so large, that a certain conclusion cannot be drawn, other than that processes (b) and (c) are both compatible with these high energy data, and process (a) is hard to reconcile with the data.

#### 4.2. The sub-Fe group

The elements scandium through manganese, Sc, Ti, V, Cr and Mn are mostly produced in the breakup of the Fe-group elements Fe, Co and Ni. Their combined spectrum is shown in Fig. 4. Here we also show the spectrum, which would result from spallation in the interstellar medium at large, using the notion that for these high energy particles the time dependence

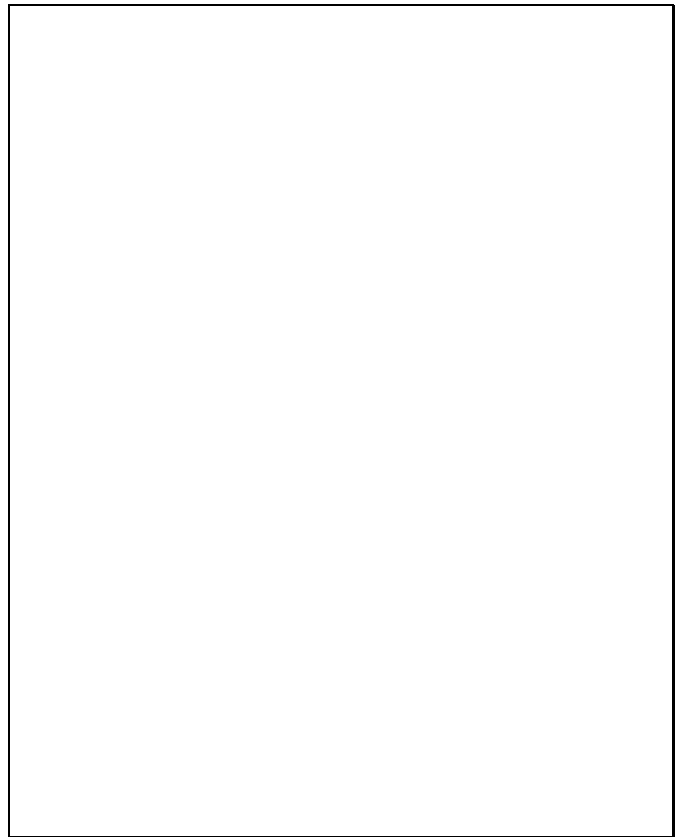


**Fig. 3.** The data of the differential fluxes for the elements Li, Be, and B including the fit for the combined flux.

of molecular clouds is no longer relevant (process (b)), but still dominant over source-related spallation (process (c)).

It seems that process (c), the source related spallation gives a much better fit to the data. But taken into account the statistical errors and systematic uncertainties involved in the data measurements, a final decision between the different models cannot be made at the moment. Within the errors, both model combinations are compatible with the data.

The spectral index for the sub-Fe elements is the same as that for the Fe-group elements, consistent with the notion that at these particle energies the spallation is dominated by source interaction.

The explanation put forward by Nath & Biermann (1994b) for the COMPTEL-observation of  $\gamma$ -ray emission lines from the Orion star forming region suggests that the interaction of the supernova shock running at first through the wind, and then hitting a shell of dense material provides a certain amount of near-source spallation of a grammage of order  $\approx 1$  gm/cm<sup>2</sup>. Here we wish to estimate this grammage from the data to check for consistency. Since the charge  $Z$  for sub-Fe and Fe-group elements are very close, it is not important whether we use in this estimate energy/charge or energy/particle; we will continue to use the latter framework.

The spallation cross section of Fe to sub-Fe is about 300 mbarn, which corresponds to a grammage of 5.6 gm/cm<sup>2</sup>, and so the ratio of  $\Phi_o$  for sub-Fe to Fe-group elements gives us  $\approx 0.19$  in numbers for an inferred grammage of order 1 gm/cm<sup>2</sup>,

quite consistent with the earlier estimate. When deriving the spallation during the transport this source-related grammage has to be subtracted.

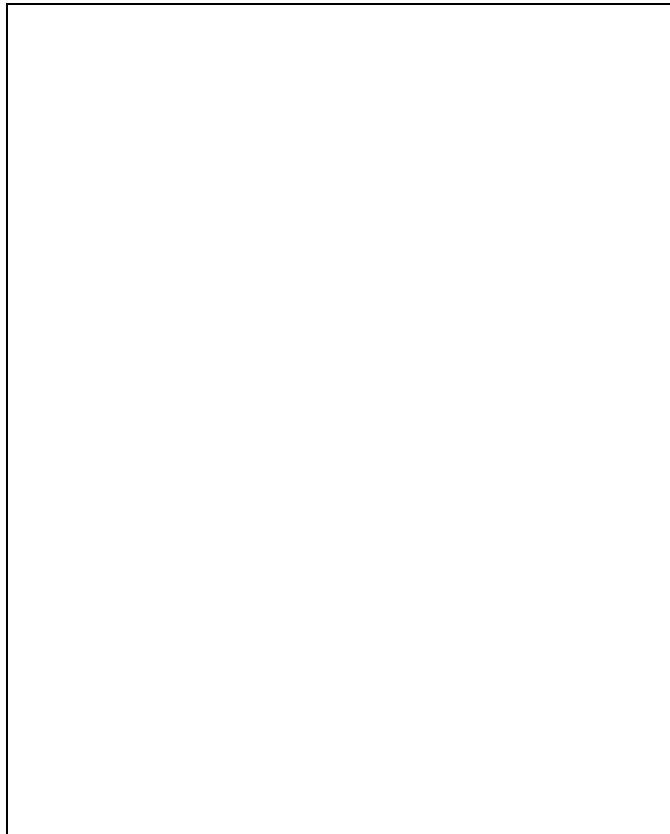


**Fig. 4.** The spectrum of the sub-Fe group elements : data, fit (solid line), pure ‘wind-SN spectrum’ (upper dashed line) and the “wind-SN spectrum” steepened by 1/3 (lower dashed line). The latter spectra are normalized at that energy where our fit begins, about 200 GeV/particle.

## 5. Summary

Here we have discussed first the predictions and the errors inherent in the theory to explain the origin of cosmic rays proposed by (paper CR I and later papers) and then give the cosmic ray spectra above 10Z GeV for all elements from  $Z = 1$  to 28, based on the full available set of data. Fitting powerlaws to the spectra we compare the powerlaw indices with the prediction.

The agreement is quite satisfactory.

The spectra imply that a substantial component of spallation exists at the source, with a grammage of order  $1 \text{ gm/cm}^2$ ; such a level of spallation can be understood from the interaction of the cosmic rays in the supernova shock as it hits a surrounding molecular shell (see Nath & Biermann 1994b).

Further work will concentrate on improving our understanding of the detailed abundances of cosmic rays.

**Acknowledgements.** High Energy Physics with author PLB is supported by a NATO travel grant (CRG 9100072). B. Wiebel-Sooth and H. Meyer are supported by the BMBF, FRG, under contract number 05 2 WT 164. PLB would like to thank Drs. G. Battistoni, T. Gaisser, P. Lipari, D. Müller, R. Protheroe, M. Shapiro, and T. Stanev for many hours of intense discussion of the topics raised in this paper.

## Appendix

**Table 4**

Element	References
H	Ryan et al. (1972), Ichimura et al. (1993a, b, c), Kawamura et al. (1990), Papini et al. (1993), Zatsepin et al. (1990), Ivanenko et al. (1987, 1990, 1993), Burnett et al. (1990a, b), Asakimori et al. (1991), JACEE (1993), Shibata (1995)
He	Ryan et al. (1972), Ichimura et al. (1993a, b, c), Kawamura et al. (1990), Papini et al. (1993), Buckley et al. (1993), Dwyer et al. (1993), Ivanenko et al. (1987, 1990, 1993), Burnett et al. (1990a, b), Asakimori et al. (1991), JACEE (1993), Shibata (1995)
Li	Orth et al. (1978)
Be	Engelmann et al. (1985, 1990), Orth et al. (1978), Buckley et al. (1993), Dwyer et al. (1993)
B	Engelmann et al. (1985, 1990), Orth et al. (1978) Júliusson (1974), Caldwell (1977), Buckley et al. (1993), Dwyer et al. (1993), Lezniak & Webber (1978), Webber (1982), Simon et al. (1980), Swordy et al. (1990, 1993), Müller et al. (1991a, b), Grunsfeld et al. (1988)
C	Engelmann et al. (1985, 1990), Orth et al. (1978), Júliusson (1974), Caldwell (1977), Buckley et al. (1993), Dwyer et al. (1993), Lezniak & Webber (1978), Webber (1982), Simon et al. (1980), Swordy et al. (1990, 1993), Müller et al. (1991a, b), Grunsfeld et al. (1988)
N	Engelmann et al. (1985, 1990), Orth et al. (1978), Júliusson (1974), Caldwell (1977), Lezniak & Webber (1978), Webber (1982), Simon et al. (1980), Swordy et al. (1990, 1993), Müller et al. (1991a, b), Grunsfeld et al. (1988)
O	Engelmann et al. (1985, 1990), Orth et al. (1978), Lezniak & Webber (1978), Webber (1982), Júliusson (1974), Buckley et al. (1993), Dwyer et al. (1993), Caldwell (1977), Simon et al. (1980), Swordy et al. (1990, 1993), Müller et al. (1991a, b), Grunsfeld et al. (1988)
F	Engelmann et al. (1985, 1990), Orth et al. (1978), Júliusson (1974), Caldwell (1977)
Ne	Engelmann et al. (1985, 1990), Orth et al. (1978), Júliusson (1974), Caldwell (1977), Simon et al. (1980), Swordy et al. (1990, 1993), Müller et al. (1991a, b), Grunsfeld et al. (1988)
Na	Engelmann et al. (1985, 1990), Orth et al. (1978), Caldwell (1977)

**Table 4 (continued)**

Element	References
Mg	Engelmann et al. (1985, 1990), Orth et al. (1978), Júliusson (1974), Caldwell (1977), Simon et al. (1980), Swordy et al. (1990, 1993), Müller et al. (1991a, b), Grunsfeld et al. (1988),
Al	Engelmann et al. (1985, 1990), Orth et al. (1978), Júliusson (1974), Caldwell (1977),
Si	Engelmann et al. (1985, 1990), Orth et al. (1978), Júliusson (1974), Caldwell (1977), Ichimura et al. (1993a, b, c), Kawamura et al. (1990), Kamioka et al. (1997), Swordy et al. (1990, 1993), Müller et al. (1991a, b), Grunsfeld et al. (1988)
P	Engelmann et al. (1985, 1990)
S	Ichimura et al. (1993a, b, c), Kawamura et al. (1990), Kamioka et al. (1997), Engelmann et al. (1985, 1990)
Cl	Engelmann et al. (1985, 1990)
Ar	Engelmann et al. (1985, 1990), Kamioka et al. (1997)
K	Engelmann et al. (1985, 1990)
Ca	Engelmann et al. (1985, 1990), Ichimura et al. (1993a, b, c), Kawamura et al. (1990), Kamioka et al. (1997)
Sc	Engelmann et al. (1985, 1990)
Ti	Engelmann et al. (1985, 1990)
V	Engelmann et al. (1985, 1990)
Cr	Engelmann et al. (1985, 1990)
Mn	Engelmann et al. (1985, 1990)
Fe	Engelmann et al. (1985, 1990), Minagawa (1981)
Co	Engelmann et al. (1985, 1990)
Ni	Engelmann et al. (1985, 1990), Minagawa (1981)
C-O	Burnett et al. (1990a, b), Asakimori et al. (1991), JACEE (1993)
Cl - Ca	Simon et al. (1980), Burnett et al. (1990a, b), Asakimori et al. (1991), JACEE (1993), Shibata (1995), Ichimura et al. (1993a, b, c), Kawamura et al. (1990), Kamioka et al. (1997)
Sc - Mn	Simon et al. (1980), Ichimura et al. (1993a, b, c), Kawamura et al. (1990), Kamioka et al. (1997)
Fe - Ni	Engelmann et al. (1985, 1990), Simon et al. (1980), Swordy et al. (1990, 1993), Müller et al. (1991a, b), Grunsfeld et al. (1988), Ichimura et al. (1993a, b, c), Kawamura et al. (1990), Kamioka et al. (1997), Burnett et al. (1990a, b), Asakimori et al. (1991), JACEE (1993), Shibata (1995)

**References**

Amenomori M., Cao Z., Dai B.Z., et al., 1996, ApJ 461, 408

Asakimori K., Burnett T.H., Cherry M.L., et al., 1991, Proc. 22nd ICRC Dublin, OG 6.1-2 and OG 6.2-9

Berezinsky V.S., Bulanov S.V., Dogiel V.A., Ptuskin V.S., 1990, *Astrophysics of Cosmic Rays*, North-Holland, Amsterdam (especially chapter IV)

Biermann P.L., 1993a, A&A 271, 649 (paper CR I)

Biermann P.L., 1993b, in "Invited and rapporteur lectures of the 23rd International Cosmic Ray Conference", Calgary, Eds. R.B. Hicks, and D. Leahy, World Scientific, Singapore, p. 45 - 83

Biermann P.L., 1993c, "Highly luminous radiogalaxies as sources of cosmic rays" in "Currents in Astrophysics and Cosmology", (Conf. proc. 1990, paper sent in 1989) Eds. G.G. Fazio, R. Silberberg, Cambridge Univ. Press, Cambridge, UK, p. 12 - 19

Biermann P.L., 1994, in "High energy astrophysics", Ed. J. Matthews, World Scientific, Singapore, p. 217 - 286

Biermann P.L., 1995a, in "Frontier objects in astrophysics and particle physics", Eds. F. Giovanelli et al., Italian Physical Society, Bologna, p. 469 - 481

Biermann P.L., 1995b, in "Proc. of the Gamow seminar in St. Petersburg", Eds. A.M. Bykov, R.A. Chevalier, Spac. Sci. Rev. 74, 385 - 396

Biermann P.L., 1996, in Proc. conference MESON96, Krakow, Eds. A. Magiera et al., Acta Phys. Polon. B 27, 3399 - 3415

Biermann P.L., 1997a, J. Phys. G 23, 1

Biermann P.L., 1997b, in "Cosmic winds and the heliosphere", Eds. J.R. Jokipii et al., Univ. of Arizona Press, (76 pages) (in press)

Biermann P.L., Cassinelli J.P., 1993 , A&A 277, 691 (paper CR II)

Biermann P.L., Strom, R.G., 1993, A&A 275, 659 (paper CR III)

Biermann P.L., Gaisser T.K., Stanev T., 1995a, Phys. Rev. D 51, 3450

Biermann P.L., Strom R.G., Falcke H., 1995b, A&A 302, 429 (paper CR V)

Biermann P.L., Kang H., Ryu D., 1997, in "Extremely high energy cosmic rays", Ed. M. Nagano, Univ. of Tokyo, (in press)

Buckley J., Dwyer J., Müller D., et al., 1993, Proc. 23rd ICRC Calgary, vol. 1, 599 - 602

Burnett T.H., Dake S., Derrickson J.H., et al., 1990a, ApJ 349, L25

Burnett T.H., Dake S., Derrickson J.H., et al., 1990b, Proc. 21st ICRC Adelaide, OG 6.1-10

Caldwell J.H., 1977, ApJ 218, 269

Drury L.O'C, 1983, Rep. Prog. Phys. 46, 973

Drury L.O'C, Aharonian F.A., Völk H.J., 1993, Proc. 23rd ICRC Calgary, vol. 1, 455 - 458

DuVernois M.A., Garcia-Munoz M., Pyle K.R., et al., 1996a, ApJ 466, 457

DuVernois M.A., Simpson, J.A., Thayer, M.R., 1996b, A&A 316, 555

Dwyer J., Buckley J., Müller D., et al., 1993, Proc. 23rd ICRC Calgary, vol. 1 , 587 - 590

Engelmann J.J., Ferrando P., Soutoul A., et al., 1990, A&A 233, 96

Engelmann J.J., Goret P., Júliusson E., et al., 1985, A&A 148, 12

Evenson P., Meyer P., 1984, J. Geophys. Res. 89, No. A5, 2647

Fermi E., 1949, Phys. Rev. 2nd ser., vol. 75, no. 8, 1169

Fermi E., 1954, ApJ. 119, 1

Garcia-Munoz M., Meyer P., Pyle K.R., Simpson J.A., 1986, J. Geophys. Res. 91, No. A3, 2858

Garcia-Munoz M., Simpson J.A., Guzik T.G., et al., 1987, ApJS 64, 269

Goldstein M.L., Roberts D.A., Matthaeus W.H., 1995, *ARA&A* 33, 283

Grunsfeld J.M., L'Heureux J., Meyer P., et al., 1988, *ApJ* 327, L31

Hess V.F., 1912, *Phys. Z.* 13, 1084

Ichimura M., Kamioka E., Kirii K., et al., 1993a, *Proc. 23rd ICRC* Calgary, vol. 2, 1 - 4, vol. 2, 5 - 8 and vol. 2, 9 - 12

Ichimura M., Kogawa M., Kuramata S., et al., 1993b, *Phys. Rev. D*, vol.48, No.5, 1949

Ichimura M., Kogawa M., Kuramata S., et al., 1993c, *Proc. 23rd ICRC* Calgary, vol. 1, 591 - 594

Ivanenko I.P., Grigorov N.L., Shestoporov V.Ya., et al., 1987, *Sov. J. Nucl. Phys.* 45 (4), 664

Ivanenko I.P., Rapoport I.D., Shestoporov V.Ya., et al., 1990, *Proc. 21st ICRC* Adelaide, OG 6.1-3

Ivanenko I.P., Shestoporov V.Ya., Chicova L.O., et al., 1993, *Proc. 23rd ICRC* Calgary, vol. 2, 17 - 20

JACEE-Collaboration, 1993, Contributions to 23rd ICRC Calgary, Louisiana State University Report, LA 70803 - 4001

Jokipii J.R., 1982, *ApJ* 255, 716

Jokipii J.R., 1987, *ApJ* 313, 842

Jokipii J.R., Levy E.H., Hubbard W.B., 1977, *ApJ* 213, 861

Júliusson E., 1974, *ApJ*, 191, 331

Kamioka E., Hareyama M., Ichimura M., et al., 1997, *Astropart. Phys.* 6, 155

Kawamura Y., Matsutani H., Nanjo H., et al., 1990, *Proc. 21st ICRC* Adelaide, OG 6.1-5 and OG 6.1-6

Kohlhörster W., 1913, *Phys. Z.* 14, 1153

Lezniak J.A., Webber W.R., 1978, *ApJ*, 223, 676

Minagawa G., 1981, *ApJ* 248, 847

Müller D., Grunsfeld J., L'Heureux J., et al., 1991a, *Proc. 22nd ICRC* Dublin, OG 6.1.12

Müller D., Swordy S.P., Meyer P., et al, 1991b, *ApJ* 374, 356

Nagano M., Hara T., Hatano Y., et al., 1984 *J. Phys. G* 10, 1295

Nath B.B., Biermann P.L., 1993, *MNRAS* 265, 241

Nath B.B., Biermann P.L., 1994a, *MNRAS* 267, 447

Nath B.B., Biermann P.L., 1994b, *MNRAS* 270, L33

Orth C.D., Buffington A., Smoot G.F., et al., 1978, *ApJ* 226, 1147

Papini P., Grimani C., Basini F., et al., 1993, *Proc. 23rd ICRC* Calgary, vol. 1, 579

Parker E.N., 1958, *ApJ*. 128, 664

Peters B., 1959, *Nuov. Cim. Suppl.* vol. XIV, ser. X, 436

Peters B., 1961, *Nuov. Cim.* vol. XXII, 800

Prandtl L., 1925, *Zeitschrift angew. Math. und Mech.* 5, 136

Prandtl L., 1949, "Guide through the theory of fluid motion (German)" Vieweg, Braunschweig, fifth ed. (1st Ed. "Abriß der Strömungslehre" 1931)

Rachen J., Biermann P.L., 1993, *A&A*. 272, 161 (paper UHE CR I)

Rachen J., Stanev T., Biermann P.L., 1993, *A&A* 273, 377 (paper UHE CR II)

Ramaty R., Kozlovsky B., Lingenfelter R.E., Reeves H., 1997, *ApJ* 488, 730

Rickett B.J., 1990, *ARA&A* 28, 561

Ryan M.J., Ormes J.F., Balasubrahmanyam V.K., 1972, *Phys. Rev. Lett.* 28, No.15, 985

Seo E.S., Ormes J.F., Streitmatter R.E., et al., 1991, *ApJ* 378, 763

Simon M., Spiegelhauer H., Schmidt W.K.H., et al., 1980, *ApJ* 239, 712

Shibata T., 1995, Rapporteur paper in "Proceedings of the 24th International Cosmic Ray Conference Rome, Invited, Rapporteurs & Highlight Papers", Eds. N. Iucci, E. Lamanna, pp. 713-736

Stanev T., Biermann P.L., Gaisser T.K., 1993 , *A&A* 274, 902 (paper CR IV)

Stanev T., Biermann P.L., Lloyd-Evans J., Rachen J., Watson A.A., 1995, *Phys. Rev. Lett.* 75, 3056

Strömgren B., 1953, in "The Sun", Ed. G.P. Kuiper, Univ. of Chicago Press, p. 36 - 87

Swordy S.P., L'Heureux J., Meyer P., et al., 1993, *ApJ* 403, 658

Swordy S.P., Müller D., Meyer P., et al., 1990, *ApJ* 349, 625

Webber W.R., 1982, *ApJ*, 255, 329

Wiebel-Sooth B., Biermann P.L., Meyer H., 1995, *Proc. 24th ICRC* Rome, vol. 3, 45 - 47

Wiebel-Sooth B., Biermann P.L., Meyer H., (paper CR VI), in prep.

Zatsepin V.I., Zamchalova E.A., Varkovitskaya A.Ya., et al., 1990, *Proc. 21st ICRC* Adelaide, OG 6.1-4

This article was processed by the author using Springer-Verlag *TEX* *AA* macro package 1989.

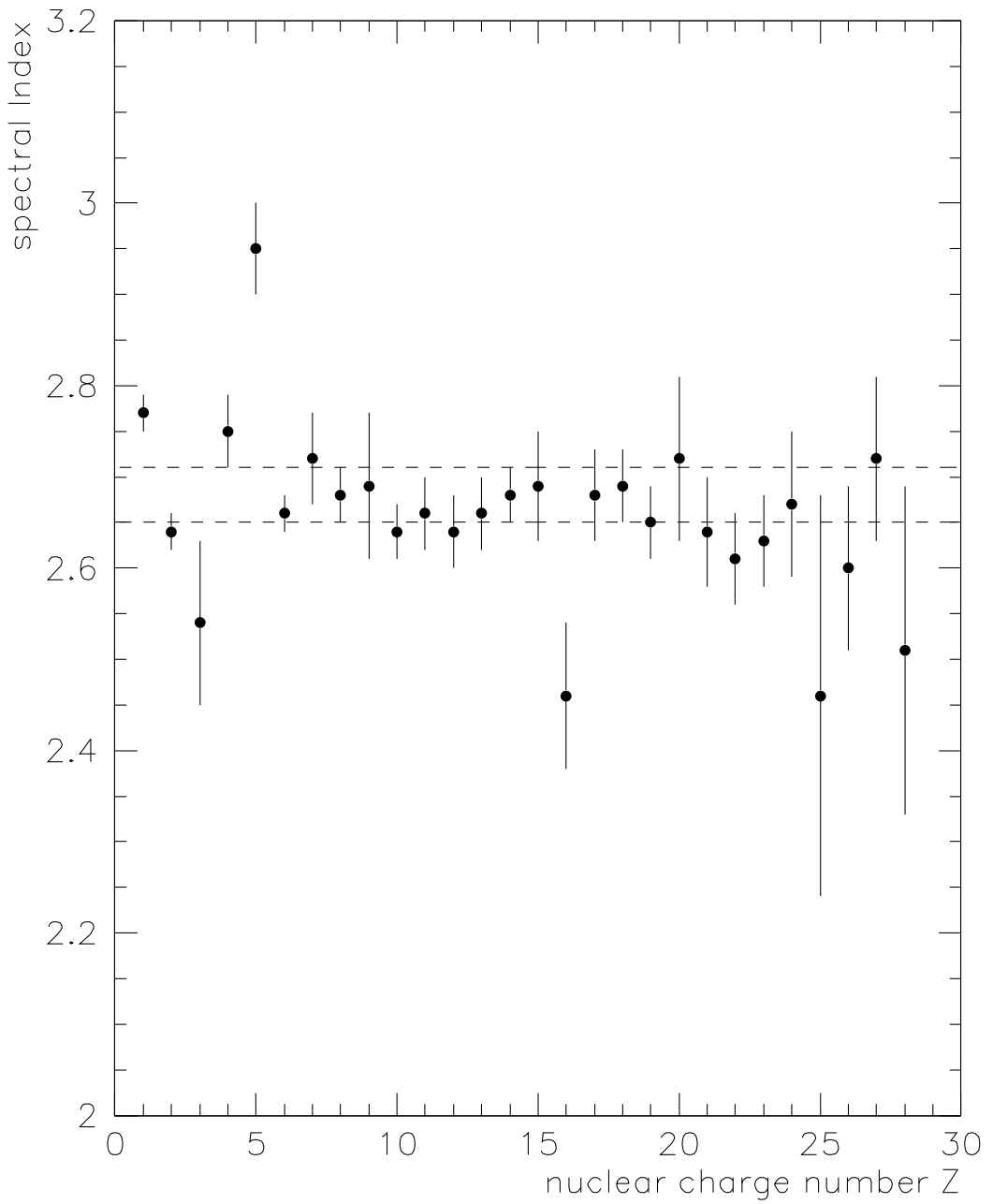


Figure 1: The spectral indices for the various elements as a function of the nuclear charge number  $Z$ . The dashed lines indicate the range of the spectral index predicted for wind-SN.

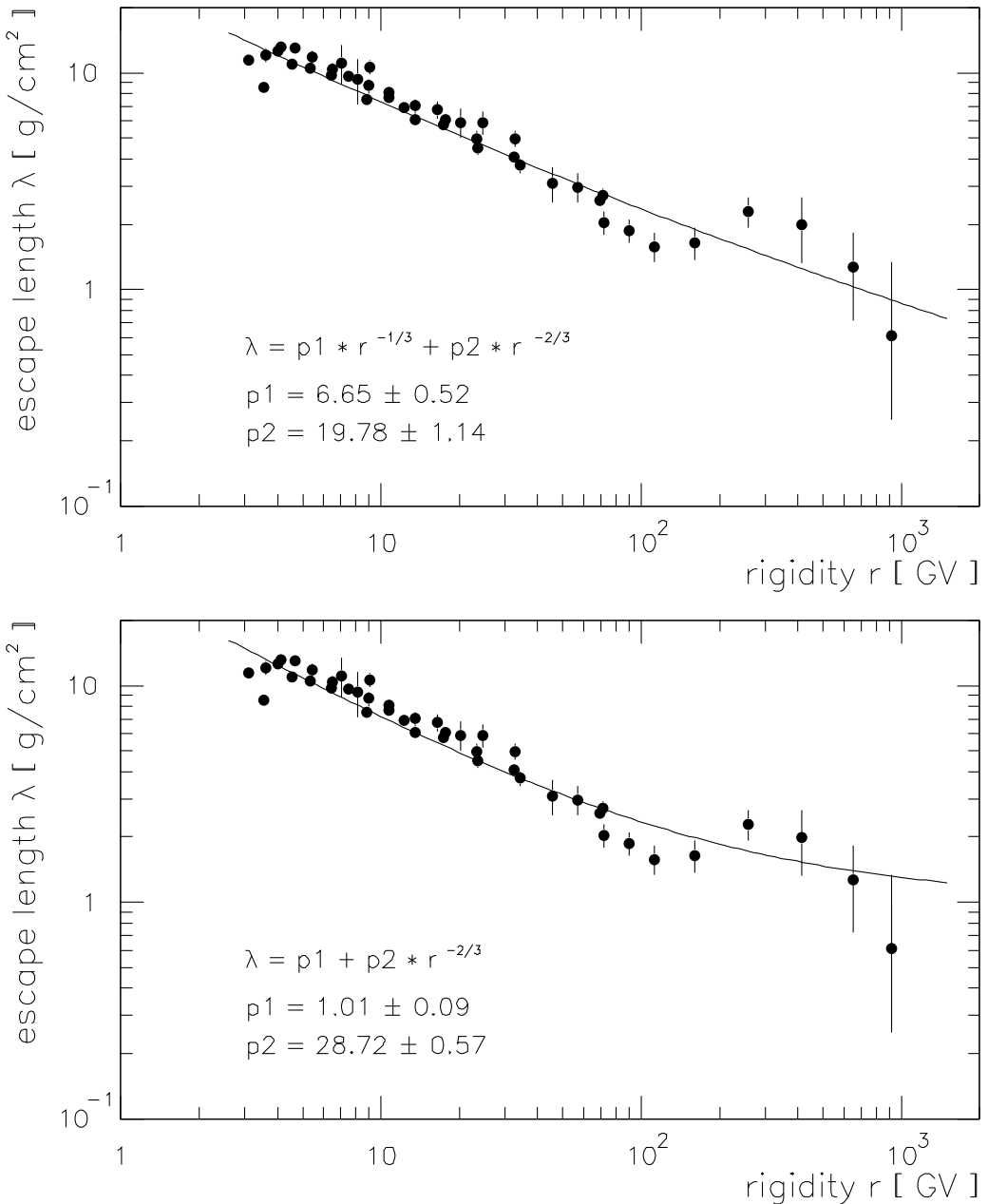


Figure 2: Here we show the data as given by Shibata (1995), and fit them with the two models explained. The top shows the combination of process (a) and (b), and the bottom shows the combination of processes (a) and (c). (For explanation see text, Sect. 4).

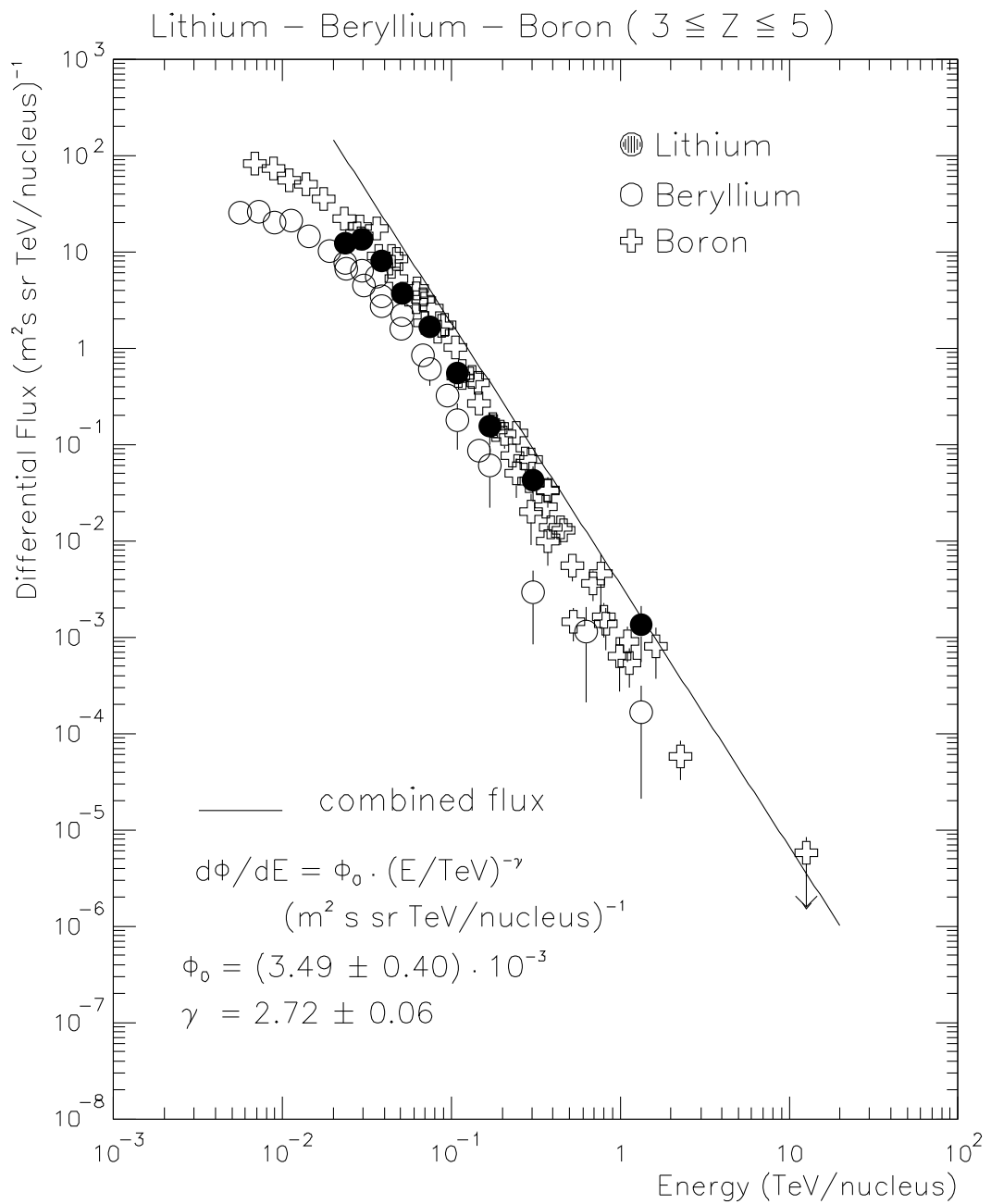


Figure 3: The data of the differential fluxes for the elements Li, Be, and B including the fit for the combined flux.

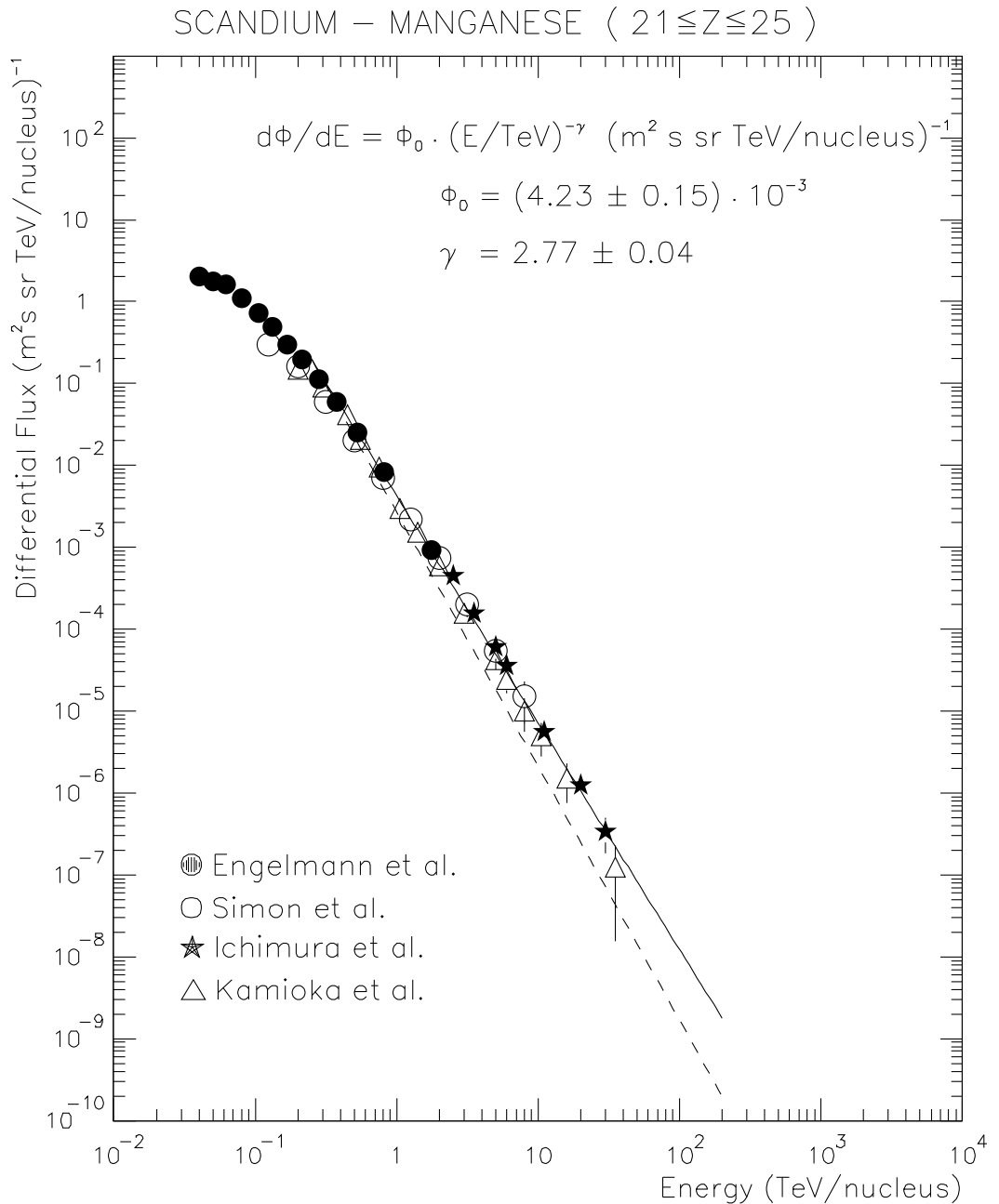


Figure 4: The spectrum of the sub-Fe group elements : data, fit (solid line), pure wind-SN spectrum” (upper dashed line) and the ‘wind-SN spectrum” steepened by 1/3 (lower dashed line). The latter spectra are normalized at that energy where our fit begins, about 200 GeV/particle.